Effects of gravity data quality and spacing on the accuracy of the geoid in South Korea

Chang-Ki Hong[1], Jay Hyoun Kwon[1], Bo Mi Lee[1], Jisun Lee[1], Yun Soo Choi[1], and Suk-Bae Lee[2]

[1]*Department of Geoinformatics, The University of Seoul, Seoul 130-743, Korea*
[2]*Department of Civil Engineering, Jinju National University, Jinju, Kyongnam 660-758, Korea*

(Received February 13, 2009; Revised April 7, 2009; Accepted April 13, 2009; Online published August 31, 2009)

The effects of gravity data quality and spacing on the accuracy of the computed geoid are analyzed. The analysis is performed using simulated gravity data that accommodate the real gravity signal in South Korea. The reference geoid is generated using both simulated gravity data and digital terrain models (DTM), assuming that both data sets are errorless. By artificially controlling the gravity data quality and spacing, we are able to calculate and analyze the geoid errors. The results show that the current distribution of real gravity data in South Korea causes geoid errors, with the standard deviation being as much as 8 cm, and that these geoid errors are mainly caused by the distribution of gravity data rather than by the noise in the data. Areas showing large geoid errors are also clearly identified; these areas should be subjected to supplementary gravity surveying at data spacing smaller than 2 km to achieve a 5-cm level of geoid accuracy.
Key words: Gravity data quality and spacing, digital terrain model, precision geoid determination.

1. Introduction

The geoid, which is the equipotential surface that best approximates the mean sea surface, is the basic element of geodetic infrastructure. The basic roles of the geoid are to represent the shape of the Earth and function as the vertical reference surface. However, it also has various applications in many scientific and engineering fields, such as the monitoring of changes in the sea level, post-glacial rebound studies, among others. Given the recent advances in technology, the Geodetic Society of Japan has set the challenging objective of developing a centimeter-level geoid, which means that the direct determination of orthometric height using satellite positioning techniques is feasible (Kotsakis and Sideris, 1999; Toth *et al*., 2000; Hwang and Hwang, 2002; Marzooqu *et al*., 2005). In terms of the large expenditure of both money and labor that are involved in conducting the traditional spirit leveling, orthometric height determination using both Global Positioning System (GPS) and the precision geoid has clear advantages.

There have been several studies on the development of the geoid over the Korean region, and approximately a 30-cm level of geoid accuracy (in terms of standard deviation) can be obtained using the gravity data that have been collected (Lee *et al*., 1996; Yun, 1995, 1999; Lee, 2000). However, most of the geodetic applications nowadays need a much higher degree of geoid accuracy. Consequently, the development of a high-precision geoid over the Korea region was planned by the Korean government in 2007. This project is now on-going and has the goal of developing a new geoid model with a 5-cm level of geoid accuracy. The first step in developing such a high-precision geoid model is to secure good quality gravity data because the geoid is determined using the Stokes' integral—i.e., the geoid is represented as a function of gravity anomaly. The selection of an optimal gravity data interval is also required to avoid a possible aliasing effect and to meet the requested geoid accuracy. This could be one of main challenges in developing a precision geoid model, especially for the South Korea region, since the surveyed gravity data are not sufficient in the mountainous areas, make up 70% of Korean territory. Therefore, supplementary gravity surveying, if necessary, should be conducted for the precision geoid once the effects of the quality and the spacing of gravity data on the computation of geoid accuracy are analyzed. However, not many studies on the effects of the quality and the spacing of gravity data on the accuracy of the geoid are available. We therefore have analyzed the effect of both gravity data quality and spacing on the computed geoid. The analysis was performed by conducting simulations in which the data quality and the spacing were artificially controlled for. The results from this study provide the achievable accuracy of the geoid with the currently available distribution of gravity data. We then examine the required gravity data quality and distribution. The areas are identified where supplementary gravity surveying are required to obtain the high-precision geoid model in South Korea region.

2. Data and Methodology

The gravity data over South Korea have been obtained by various organizations with different instruments for more than 20 years. These data can be grouped into two categories: (1) raw data (readings from gravimeter); (2) free-air anomaly data but without raw data. For the quality control of the former dataset in the form of raw data from gravime-

Copyright © The Society of Geomagnetism and Earth, Planetary and Space Sciences (SGEPSS); The Seismological Society of Japan; The Volcanological Society of Japan; The Geodetic Society of Japan; The Japanese Society for Planetary Sciences; TERRAPUB.

Table 1. Statistics of the datasets used in this study.

	Number of points	Mean	Standard deviation	Maximum	Minimum
Free-air from datasets with raw reading (mGal)	6,878	15.01	14.85	104.25	−18.83
Free-air from datasets without raw reading (mGal)	2,112	27.14	19.95	153.89	−26.05
Simulated gravity anomaly (mGal)	324,600	11.31	18.14	210.12	−116.58
SRTM DTM (m)	8,645,901	72.28	181.81	1890.50	−4.50

Table 2. Analysis strategies adopted in this study.

Output		Gravity anomaly		DTM	
		Noise level (mGal)	Distribution type	Noise level (m)	Grid size (km)
Reference geoid		0	1-km grid	0	0.2
Geoid errors	Scenario #1	0	Current distribution	0	
	Scenario #2	0.5 1 3	Current distribution	0	
	Scenario #3	0	2-km grid 5-km grid 10-km grid	0	
	Scenario #4	0.5	Current distribution + additional 2-km grid	20	

ters, the data are re-preprocessed in a consistent manner so that free-air anomalies with a precision of 0.48 mGal are obtained (Lee *et al.*, 2008). However, the quality of the latter dataset in the form of free-air anomaly cannot be fully verified since the raw measurements of gravity data are not available. Therefore, a correlation analysis using both the global potential model (EGM96) and the terrain models is performed to detect and remove the outliers in the gravity anomaly. This is followed by the generation of the gridded gravity anomaly with a 1-km interval through a simulation with the digital terrain model (DTM) (a 0.2-km grid of land elevations) from the Shuttle Radar Topography Mission (SRTM) and the datasets described above.

The simulation procedures used to generate the gravity anomaly data can be summarized into two steps: the first step is the generation of the gravity anomaly by computing the topographic effect on the gravity using Helmert condensation; the second step is the fitting of the simulated gravity anomaly to the real one. In the Helmert condensation, a two-dimensional mass layer is assumed, then the Fourier transform of the gravity anomaly (Δg) due to the mass layer with assumption of Airy's isostatic compensation can be expressed as:

$$\Delta g = 2\pi G\rho\mathcal{F}^{-1}\left(\mathcal{F}(H)\left(1-e^{-2\pi\mu D}\right)e^{-2\pi\mu x_3}\right), \quad (1)$$

where $\mathcal{F}$ and $\mathcal{F}^{-1}$ are the operators of the forward and inverse Fourier transform, respectively; G is the gravitational constant; ρ is the density of the layer; D is the depth of isostatic compensation; x_3 is the vertical coordinate of the computation point; $\mu = \sqrt{\mu_1^2 + \mu_2^2}$ and μ_1, μ_2 are spatial frequencies on the geoid. Equation (1) states that the gravity anomaly can be simulated with height information under the assumption of Helmert condensation and Airy's isostasy. For height, the SRTM grids of the 200-m interval are used. After the gravity anomaly is simulated based on Eq. (1), the simulated gravity is fitted to the real gravity as follows. First, a Triangulated Irregular Network (TIN) is constructed using real gravity data. Second, the grid points of the simulated gravity inside the TIN are identified, and plane fitting is performed in order to calculate the residual at each grid point. Finally, the plane from the simulated gravity is removed, and the plane from the TIN is added to the residual calculated in the previous stage. In this way, the simulated gravity anomaly is now fitted to the real gravity anomaly to some degree so that the possible biases on the simulation are removed. More details on the procedures used for generating the gravity anomaly data can be found in Jekeli (2003). The statistical characteristics of the datasets used in this study are shown in Table 1. Note that the standard deviation of the simulated gravity anomaly falls between those of the two datasets, with/without raw reading, and shows some degree of consistency to real gravity data.

The simulated gravity anomaly together with DTM is now used to compute the geoid with a 2-km spatial resolution, and this geoid is assumed to be an error-free "reference geoid". The geoid errors due to the noises in the gravity anomaly are subsequently analyzed with the current distribution of gravity data. The effects of both the qualities and the spacings of gravity data on the accuracy of the computed geoid are also investigated. Finally, the supplementary gravity surveying plan to be made for the improvement of geoid accuracy is provided based on the numerical results. Table 2 shows the summary of analysis strategies adopted in this study. The qualities and spacings of data are controlled by adding different levels of Gaussian random noise and by selecting different spatial intervals, respectively. Consequently, the impacts of data quality and the spacing of gravity anomaly data on the accuracies of computed geoid can be analyzed.

The computation of the geoid is performed using the Gravsoft software developed by Tscherning *et al.* (1992). This means that the global geopotential model, i.e., EGM96, is used for the modeling of the long wavelength of

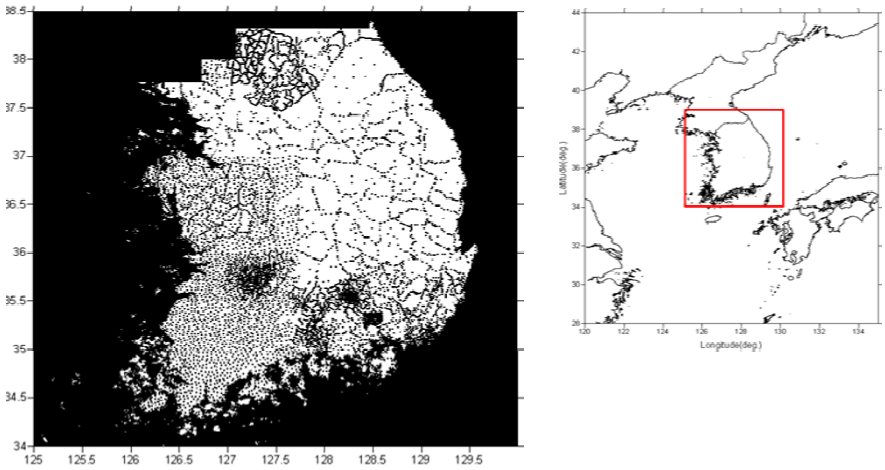

Fig. 1. Distribution map of real gravity data over the South Korea.

the Earth's gravity field. The gravity data on both land and sea are used for the modeling of the medium wavelength, with the DNSC08 model from the Danish National Space Center used for altimetry data over the sea and DTM for the short wavelength of the gravity signal over the land area. The Remove-Restore (R-R) technique is applied to generate the gravimetric geoid. Finally, this gravimetric geoid is fitted to the GPS/Leveling data so that the possible bias due to the local datum is removed.

3. Results

3.1 Simulated gravity anomaly and the geoid

To analyze the effects of both qualities and spacings of both gravity and DTM on the accuracy of the computed geoid, we create the reference geoid using the simulated gravity anomaly and DTM. The simulated gravity anomaly with the incorporation of real gravity data is obtained as a regular grid with a mesh size of 1×1 km. As explained in Section 2, the incorporation of real gravity data is performed so that the simulated gravity anomaly can reflect the characteristic of the real gravity anomaly as much as possible. Figure 1 shows the location map of the real gravity data over South Korea, with each black dot indicating the measurement point. As can be seen in Fig. 1, the measurement points are densely located on the southwestern part of South Korea, while sparse distributions are observed on the eastern part, which corresponds to the mountainous area. Therefore, it is expected that the geoid errors occur dominantly in the mountainous area.

Also, the DTM from the SRTM is gridded on a regular 0.2×0.2-km grid. The gridding of STRM is simply carried out by extracting every other data because SRTM is already in a grid format. Once gravity anomaly and DTM data are obtained, the geoid is computed as explained in Section 2. Figure 2 presents the computed geoid—i.e., reference geoid—using the simulated gravity anomaly with a 1-km grid size and a DTM with a 0.2-km grid size. As shown in Fig. 2, the geoid variation ranges from 21 to 30 m, gradually increasing from the northwest to southeast part of South Korea.

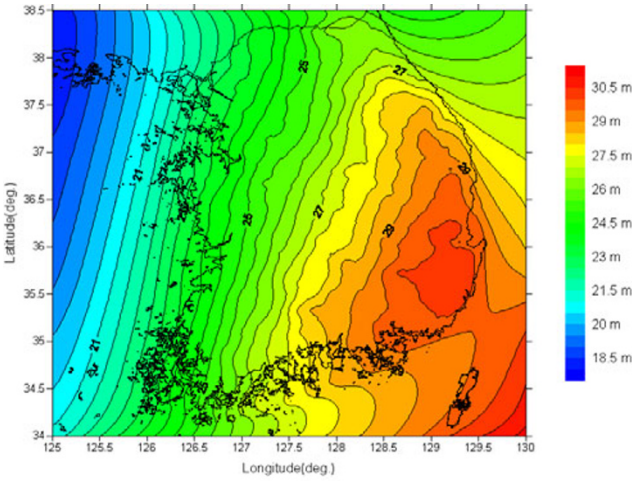

Fig. 2. Simulated geoid over the South Korea.

3.2 Geoid errors due to the current distribution of gravity data

To analyze the geoid errors due to the current distribution of gravity data, linear interpolation is applied to the simulated gravity anomaly (with a 1-km grid size) so that the gravity anomaly is obtained at each location where real gravity data is available. The primary objective of this analysis is to examine geoid errors due to the current distribution of gravity data; consequently, the gravity anomaly and the DTM are assumed to be errorless. The geoid is generated using the gravity anomaly with the current distribution and the DTM. The geoid errors are then obtained by computing the difference between the reference and the computed geoid at each grid point. Figure 3 shows the geoid errors due to the current distribution of gravity data: relatively large geoid errors can be observed in the area where the gravity anomaly data are sparsely distributed. The mean and the standard deviation of the geoid errors are -1 cm and 8 cm, respectively. It should be noted that both the mean and the standard deviation are computed using the geoid er-

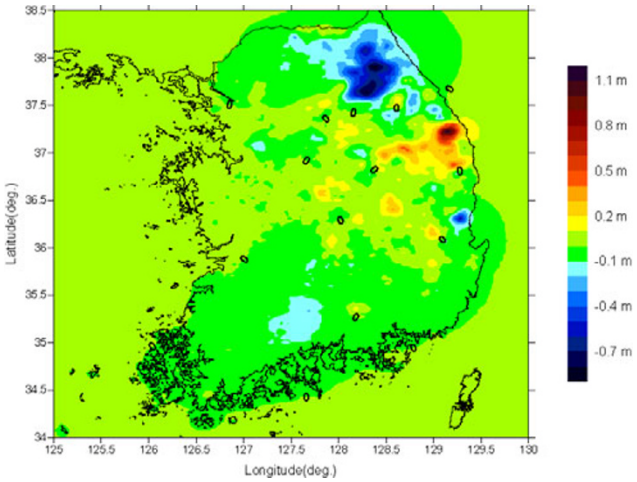

Fig. 3. Geoid errors due to the current distribution of gravity data (scenario no. 1).

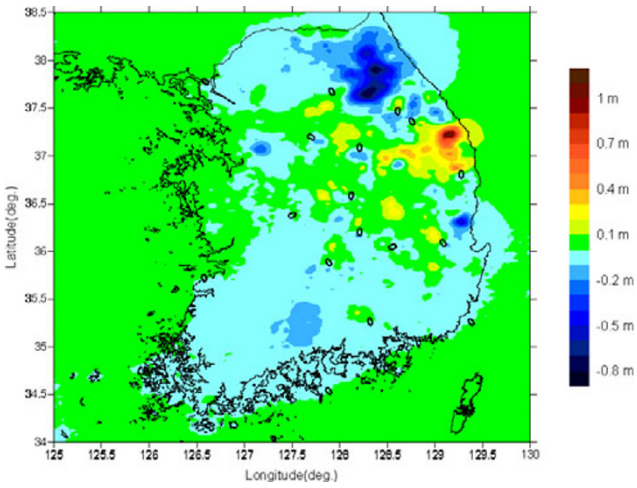

Fig. 4. Geoid errors due to the 3-mGal noise in the gravity anomaly (scenario no. 2).

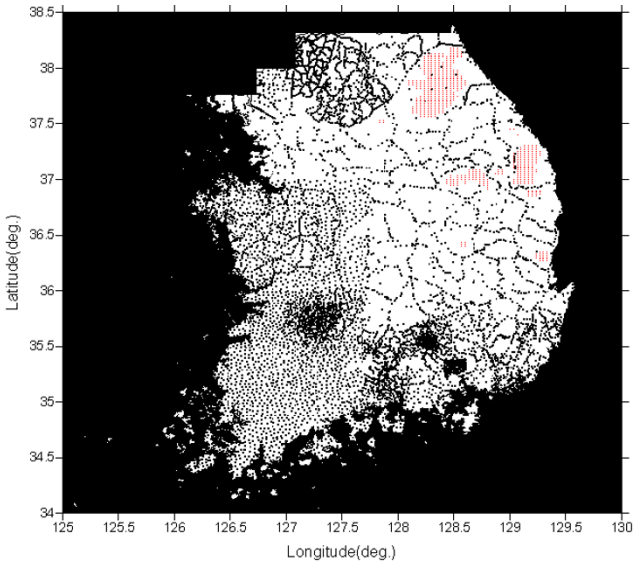

Fig. 5. Location map of supplementary gravity data.

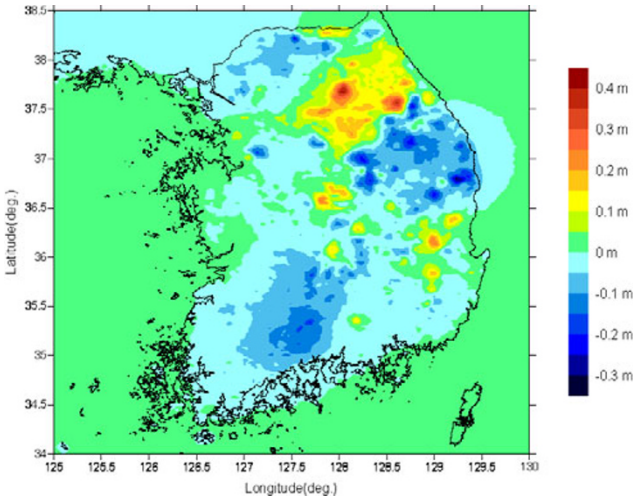

Fig. 6. Geoid errors from the supplementary gravity data (with a 2-km grid size) together with the currently distributed gravity data (scenario no. 4).

rors observed only in the South Korea region.

This result indicates that the target geoid accuracy—i.e., 5 cm—cannot be obtained using the current distribution of gravity data even though the error-free gravity anomaly and DTM are used for the data processing. However, the obtainable accuracy of the gravity anomaly is limited in the real world. This means that the effect of Gaussian random noises in the gravity anomaly on the computed geoid should be assessed in order to determine the tolerable accuracy of gravity anomaly for the development of the precision geoid. For this analysis, three gravity anomaly datasets with different noise levels are generated. In other words, Gaussian random noises with 0.5, 1, 3 mGal standard deviations are added to the simulated gravity anomaly. The geoid is then generated using each dataset as described above, and the corresponding geoid errors are computed. The results from this analysis show that the geoid errors are almost same as those shown in Table 3.

Consequently, Fig. 4, which expresses the geoid errors when 3 mGal Gaussian random noise is added to the gravity anomaly, is presented as a representative of all errors. As can be seen in Fig. 4, similar patterns and magnitudes of geoid errors as those shown in Fig. 3 are observed. This means that the geoid errors are mainly caused by the distribution of the gravity anomaly rather than the noise in the gravity anomaly. Also, we can conclude that the current quality of the gravity data is sufficient to produce the precision geoid since the quality of gravity data re-preprocessed has a precision of 0.48 mGal, as mentioned in Section 1. However, more gravity surveying should be conducted for the improvement of geoid accuracy. The remaining question is then what gravity data spacing is required and which area should be surveyed to obtain the target accuracy for the geoid. For these questions, a more detailed analysis is necessary, as follows.

3.3 Geoid errors due to the gravity data spacing

Determination of the optimal gravity data spacing is essential because the selection of gravity data spacing for the precision geoid is a trade-off between the precision of the

Table 3. Statistical characteristics of geoid errors due to the noises in the gravity data.

Noise level (mGal)	Geoid errors			
	Mean (m)	Standard deviation (m)	Maximum (m)	Minimum (m)
0.5	−0.01	0.08	1.17	−0.87
1	−0.01	0.08	1.11	−0.85
3	−0.01	0.08	1.15	−0.82

Table 4. Statistical characteristics of geoid errors due to the different gravity data spacings (scenario #3).

Gravity data spacings (km)	Geoid errors			
	Mean (m)	Standard deviation (m)	Maximum (m)	Minimum (m)
2	0.00	0.01	0.08	−0.08
5	0.00	0.02	0.19	−0.21
10	0.00	0.06	0.34	−0.61

geoid and the surveying cost. Hence, the effect of gravity data interval on the computed geoid is investigated in this section for the planning of supplementary gravity surveying if required. For the analysis, the simulated gravity anomaly datasets with a grid size of 2, 5, and 10 km, respectively, are generated, as described in Section 2. The geoid error for each data interval is computed, and its statistical characteristics of geoid errors are as shown in Table 4.

As can be expected, the geoid errors increase as the data spacing gets larger. The geoid errors reach up to 6 cm in standard deviation when a 10-km data spacing is selected for the data processing. This result indicates that the gravity data spacing should be less than 10 km to obtain the target accuracy of geoid.

3.4 Improvement of geoid accuracy with supplementary gravity data

The geoid errors due to the current distribution of gravity anomaly have already been demonstrated in Section 3.2, and the numerical result shows that an 8-cm level of geoid accuracy can be obtained. This geoid accuracy is not sufficient to obtain the precision geoid; therefore, supplementary gravity surveying should be planned and conducted to improve the geoid accuracy. In this section, predictable geoid errors are computed by adding supplementary gravity data to the location where relatively large geoid errors are observed (see Fig. 3). In other words, gravity anomaly data, located in the area where the geoid error exceeds 30 cm, are extracted from the simulated gravity anomaly. Note that 0.5-mGal noises are added to the gravity anomaly so that the accuracy of the real gravity data is properly accounted for. Figure 5 shows the locations of the supplementary gravity data point (red dot) together with the currently distributed gravity data point (black dot).

Using the gravity data shown in Fig. 5, the geoid is generated and the corresponding geoid errors are obtained, as shown in Fig. 6. The mean and the standard deviation of the geoid errors are 0 and 0.05 m, respectively. It can therefore be said that it is clearly expected that a 5-cm geoid accuracy is definitely achievable provided that supplementary gravity surveying is carried out.

4. Conclusion

The effects of both gravity data quality and spacing on the accuracy of the computed geoid over the South Korea region are analyzed in this paper. The geoid errors due to the current distribution of gravity data are also investigated so that the supplementary gravity surveying plan can be made to obtain the 5-cm level of geoid accuracy. Based on the results of the analyses carried out in this study, we conclude that the effect of gravity data spacing is larger than that of data quality on the geoid accuracy and demonstrate that the acceptable magnitude of gravity measurement errors is 3 mGal for the 5-cm level of geoid accuracy. We have clearly identified the areas in which supplementary gravity surveying is required. Finally, we recommend collecting gravity data with less than a 2-km interval for the supplementary gravity surveying in order to develop a high-precision geoid. Although the analysis presented in this study is numerically oriented, it is expected that the results will contribute to the development of the precision geoid.

Acknowledgments. This research was supported by a grant (07KLSGC02) from the Cutting-edge Urban Development-Korean Land Spatialization Research Project funded by Ministry of Land, Transport and Maritime Affairs.

References

Hwang, C. and L. Hwang, Use of geoid for assessing trigonometric height accuracy and detecting vertical land motion, *J. Surv. Eng.*, **128**(1), 1–20, 2002.

Jekeli, C., Statistical analysis of moving-base gravimetry and gravity gradiometry, OSU Report No. 466, Department of Civil and Environmental Engineering and Geodetic Science, The Ohio State University, 2003.

Kotsakis, C. and M. G. Sideris, Study of the gravity field spectrum in Canada in view of cm-geoid determination, Joint Meeting of the International Gravity Commission and the International Geoid Commission No2, Trieste, ITALIE (07/09/1998) 1999, 40(3–4), 451 p., (10 ref.), 179–188, 1999.

Lee, J. S., B. M. Lee, J. H. Kwon, and Y. W. Lee, Free-air anomaly from a consistent preprocessing of land gravity data in South Korea, *Korean J. Geomatics*, **26**(4), 379–386, 2008.

Lee, S. B., A study on the Geoid Modeling by Gravimetric Methods and Methods of Satellite Geodesy, *J. Korean Soc. Geodyn., Photogramm. Cartogr.*, **18**(4), 359–367, 2000.

Lee, S. B., H. S. Yun, and J. H. Choi, Gravimetric geoid determination by Fast Fourier Transform in and around Korean peninsula, *J. Korea Soc. Geodyn., Photogramm. Cartogra.*, **14**(1), 49–58, 1996.

Marzooqu, Y. A., H. Fashir, S. I. Ahmed, R. Forsberg, and G. Strykowski, Progress Towards a cm Geoid for Dubai Emirate, FIG Working Week 2005 and GSDI-8, Cairo, Egypt, 16–21 April 2005, 2005.

Toth, G. Y., S. Z. Rozsa, V. D. Andritsanos, J. Adam, and I. N. Tziavos, Towards a cm-geoid for Hungary: recent efforts and results, *Phys. Chem. Earth Part A*, **25**(1), 47–52, 2000.

Tscherning, C. C., R. Forsberg, and P. Knudsen, The GRAVSOFT package for geoid determination, Continental Workshop on the Geoid in Europe, May 1992, 327–334, Research Institute of Geodesy, Topography and Cartography, Prague, 1992.

Yun, H. S., Results of the geoid computation for Korean peninsula, Ph.D. dissertation, Technical University of Budapest, Hungary, 1995.

Yun, H. S., Precision geoid determination by spherical FFT in and around the Korean peninsula, *Earth Planets Space*, **51**(1), 13–18, 1999.

C.-K. Hong, J. H. Kwon (e-mail: jkwon@uos.ac.kr), B. M. Lee, J. Lee, Y. S. Choi, and S.-B. Lee